Hardened properties of high-performance printing concrete

Hardened properties of high-performance printing concrete

T. T. Le, S. A. Austin, S. Lim, R. A. Buswell, R. Law A. G. F. Gibb, T. Thorpe

Department of Civil and Building Engineering, Loughborough University, Loughborough, Leicestershire, LE11 3TU, United Kingdom

Abstract

This paper presents the hardened properties of a high-performance fibre-reinforced fine-aggregate concrete extruded through a 9 mm diameter nozzle to build layer-by-layer structural components in a printing process. The printing process is a digitally controlled additive method capable of manufacturing architectural and structural components without formwork, unlike conventional concrete construction methods. The effects of the layering process on density, compressive strength, flexural strength, tensile bond strength and drying shrinkage are presented together with the implication for mix proportions. A control concrete (mould-cast specimens) had a density of approximately 2,250 kg/m^3, high strength (107 MPa in compression, 11 MPa in flexure) and 3 MPa in direct tension, together with a relatively low drying shrinkage of 175 microns (cured in water) and 855 microns (cured in a chamber at 20^{o}C and 60% relative humidity) at 184 days. In contrast well printed concrete had a density of 2,350 kg/m^3, compressive strength of 75-102 MPa, flexural strength of 6-17 MPa depending on testing direction, and tensile bond strength between layers varying from 2.3-0.7 MPa, reducing as the printing time gap between layers

increased. The well printed concrete had significantly fewer voids greater than 0.2mm diameter (1.0%) when compared with the mould-cast control (3.8%), whilst samples of poorly printed material had more voids (4.8%) mainly formed in the interstices between filaments. The additive extrusion process was thus shown to retain the intrinsic high performance of the material.

Key words: Additive Manufacturing; Bond Strength (C); Compressive Strength (C); High-Performance Concrete (E); Tensile Properties (C)

1. Introduction

A high performance printing concrete has been developed for an innovative freeform-construction concrete-printing process [1, 2]. The concrete used some advantages of self-compacting concrete [3, 4] and sprayed concrete [5, 6] for optimisation of the mix proportions to suit the innovative process. The concrete printing process and the fresh properties of the concrete, including the optimisation of mix proportions, extrudability, workability, open time and buildability are reported elsewhere [7, 8].

The concrete printing process uses an additive, layer-based, manufacturing technique to build complex geometrical shapes without formwork and thus has a unique advantage over conventional construction methods. Additive manufacturing (AM) has been applied to the production of cement composites such as Contour Crafting [9] and D-Shape (Monolite) [10]. Contour Crafting is based upon extruding a cement-based paste against a trowel that creates a smooth surface finish through the

build up of subsequent layers. The D-Shape involves a powder deposition process, where each layer of build material is deposited to the desired thickness, compacted and then nozzles mounted on a gantry frame deposit the binder where the part is to be made solid. Other applications of AM include the medical field XXXX [11-13]. Work to overcome the poor water resistance of commercially available materials , which is problematic for applications including biomedical processing [13].

Briefly, in the concrete printing process, components are designed as volumetric objects using 3D modelling software. They are sliced and represented as a series of two dimensional layers. The data are exported to a printing machine layer-by- to print structural components by the controlled extrusion of a concrete. The rheology must allow its extrusion through a printing head incorporating a 9 mm diameter nozzle to form small concrete filaments. As they are laid, the filaments bond together to form each layer and to the previous layers to build 3D components.

The layered structure is likely to be anisotropic as voids can form between filaments to weaken the structural capability. The bond between filaments, as well as between layers, probably influences the hardened properties of concrete components. Therefore, a high strength in compression and flexure as well as tensile bond are the main targets in developing this concrete. Additionally, a low shrinkage is essential as the freeform components are built without formwork and this could accelerate water evaporation in the concrete and result in cracking.

This paper presents the hardened properties comprising density, compressive and flexural strengths, tensile bond strength and drying shrinkage. Void measurement

was also carried out to further understand the hardened properties. It compares the performance of conventionally cast (the control) and in-situ printed states, considering where appropriate the anisotropy resulting from the extrusion process.

2. Experimental Programme

2.1. Specimen manufacture

In this research, the specimens were manufactured in both mould-cast and printed states. The test results would show clearly the impact of the concrete printing process on the hardened properties of concrete.

2.2.1. Mould cast control samples

All control specimens were cast in moulds and complied with the respective BS EN standards used to measure the properties. Compressive strength specimens were cast in 100mm cube steel moulds complied with BS EN 12390-3:2009 [14]. Flexural strength specimens were cast in 100x100x500 mm steel moulds complied with BS EN 12390-5:2009 [15]. Tensile strength specimens were cored from 150mm mould-cast cubes to comply with BS EN 14488-4:2005+A1:2008 [16]. Shrinkage specimens were cast in 75x75x220mm steel moulds in accordance with BS EN 12617-4:2002 [17].

2.2.2. Printed samples

The printed specimens were manufactured by sawing and coring from printed components including 350x350x120 mm slabs, 500x350x120mm slabs, a trial curvy-shape bench with 2000/1000/63 mm length/width/thickness and 500x100x200 mm beams (see Experimental section).

As expected, the process had the potential to create small voids in the interstices between the filaments (Figure 1(a)). A cross section of a poorly manufactured specimen is shown in Figure 1(b). Careful design and control of the mix rheology and printing process avoids such macro effects, but the sample serves to illustrate the potential for longitudinal flaws and the resulting anisotropy that this paper explores.

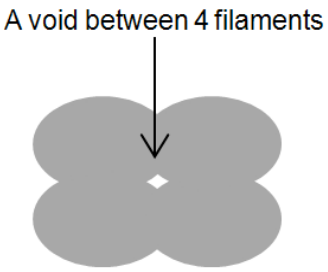

a) Four filaments may form a void

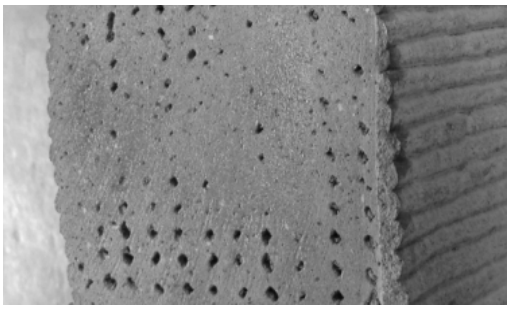

b) Poor printing example with obvious voids between filaments

Figure 1. Voids formed between filaments resulting from a poorly executed printing process

2.2. Materials and mix proportions

The mix design aimed to meet the requirements of both the fresh and hardened states. The former comprises printability, workability, open time and buildability. The hardened performance includes the compressive and flexural strengths of both cast and printed specimens. The mix design targeted a compressive strength of over 100 MPa and a flexural strength of over 10 MPa at 28 days for mould-cast specimens. A 2 mm maximum size sand was selected because of the small nozzle diameter (9mm) required to give a high printing resolution; cement CEM I 52.5, fly ash conforming to BS EN 450 and undensified silica fume formed the binder component. The gradings of sand, cement, fly ash and silica fume, measured by a Mastersizer 2000 machine, were combined in various proportions to form smooth grading curves of potential mixtures.

Dry components were mixied with water and a polycarboxylate-based superplasticiser to lower the water/binder ratio and hence increase its workability and strength. A retarder, formed by amino-tris (methylenephosphonic acid), citric acid and formaldehyde, maintained sufficient open time, facilitating a constant flow during printing. The concrete also contained 12/0.18 mm length/diameter polypropylene micro fibres to reduce the possibility of plastic shrinkage. The optimum mix was found to be one with the lowest content of binder that could be printed and built with the recommended dosage of fibres from the supplier (i.e. 1.2 kg/m^3) that gained the target strengths.

The optimisation process resulted in a mix with a 60:40 sand:binder ratio, comprising 70% cement, 20% fly ash and 10% silica fume, plus 1.2 kg/m^3 micro polypropylene

fibres [7, 8]. The water:binder ratio was 0.26. This mix required 1% superplasticiser and 0.5% retarder to attain an optimum workability of 0.55 kPa shear strength, an optimum open time of up to 100 minutes and the ability to build a large number of layers with various filament groups. The compressive strength of this mix, determined by casting 100 mm cube specimens, was 20, 80, 107 and 125 MPa, at 1, 7, 28 and 56 days respectively. A variety of parts were printed with mould-cast controls, and specimens extracted to determine the effects of this AM process on key properties, namely density, compressive strength, flexural strength, tensile bond strength and drying shrinkage. Except where stated, all properties reported are with these mix proportions.

2.3. Experimental procedures

2.3.1. Density

The density of mould-cast and printed specimens were averaged from at least three specimens, the former complying with BS EN 12390-7:2009 [18]. For printed concrete, 100 mm cube specimens were sawn from 350x350x120 mm and 500x350x120 mm printed slabs to measure the density as for the mould-cast specimens. The results were verified with 58 mm diameter cores in the investigation of tensile bond strength.

2.3.2. Compressive strength

Compressive strength was measured in both mould-cast and printed specimens. Most specimens were 100 mm cubes. Mould-cast specimens were cured in a 20^{o}C water tank and tested at 1, 7 and 28 day ages to monitor the strength development with time.

For printed elements, 100 mm cube specimens were extracted from one 350x350x120 mm slab and three 500x350x120 mm slabs (Figures 2 and 4). The slabs were cured under damp hessian, wrapped in plastic sheeting. Nine cubes were extracted from the 350x350x120 mm slab and loaded in one of three directions: direction I for specimens 1-3; direction II for specimens 4-6; and direction III for specimens 7-9 (Figure 2). Nine cubes extracted from three 500x350x120 mm slabs were tested at the same loading directions of the flexural beam specimens (Figure 4).

All 100 mm cube specimens were tested in accordance with BS EN 12390-3:2009 [14]. Printed specimens were capped with a high strength gypsum-based plaster.

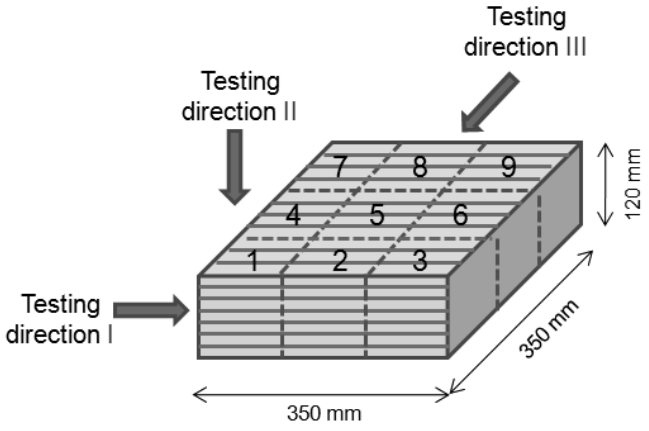

Figure 2. Cutting diagram and testing directions for nine 100 mm cube specimens extracted from the 350x350x120 mm slab.

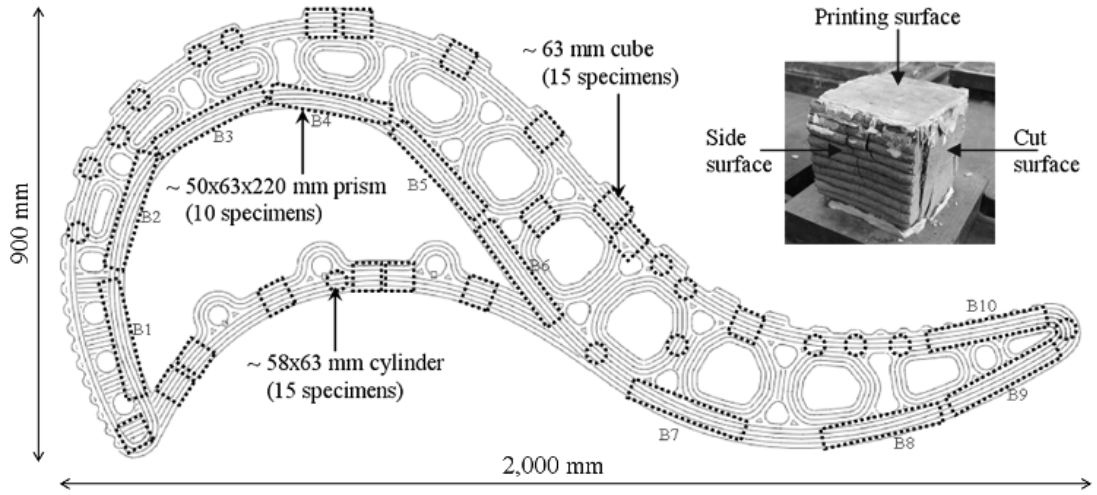

Figure 3. Diagram showing positions of extracting printed specimens from a multi-cellular curved bench and typical cube specimen

Additionally, fifteen 58 mm diameter cores, fifteen 63 mm cut cubes and ten 50 x 220 mm width x length prisms were extracted from a 63 mm thick trial print of a curved component to understand the performance of printed concrete under compressive and flexural loading (Figure 3). All cylinder were tested perpendicular to the printing surface while cube specimens were tested in three orientations: 3 perpendicular with a cut surface (loading direction I), 9 perpendicular to the printing surface (loading direction II) and 3 perpendicular with a side surface (loading direction III), as shown top-right of Figure 3. The loading rate was also 0.4 N/mm^2. The full-scale print of the bench has been shown in elsewhere [7, 8].

2.3.3. Flexural strength

Flexural strength was also measured in both mould-cast and printed states. 100x100x500 mm slabs were mould-cast, removed after one day and then cured in a 20°C water tank up to 28 days. For printed specimens, three 500x350x120 mm slabs were printed and cured under damp hessian. Three 100x100x400 mm beams and three 100 mm cubes were extracted from each slab at 28 day age. Slabs 1 and 2 were printed and cut as depicted in Figure 4a while slab 3 was printed and cut as depicted in Figure 4b. Cube and beam specimens extracted from slabs 1, 2 and 3 were tested in directions I, II and III, respectively.

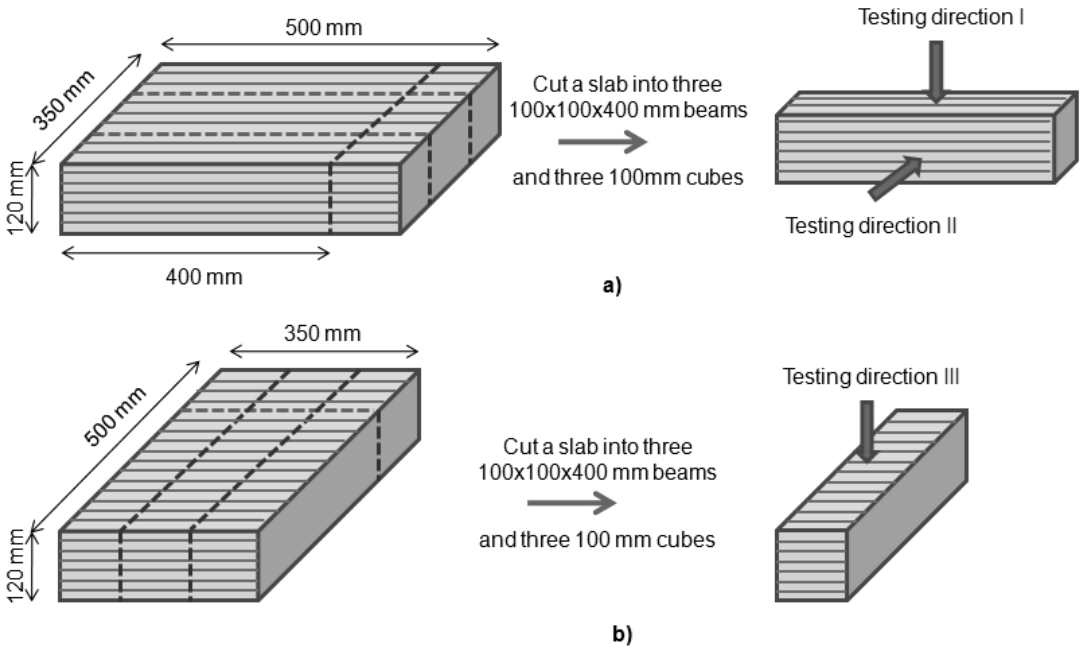

Figure 4. Diagram of cutting slabs and testing flexural strength

All beam specimens were tested under 4-point bending with a span of 300 mm, complying with BS EN 12390-5:2009 [15].. An additional ten 50x63x220 mm beam

specimens extracted from the trial printed component (Figure 3) were also tested to further understand anisotropy of the flexural performance of printed concrete.

2.3.4. Tensile bond strength

A critical characteristic of this printing process is the bond between layers, which can influence the structural performance, particularly when the process temporarily stops between layers. The influence of time between printing layers was investigated (in increments of 15, 30 minutes, 1, 2, 4, 8, 18 hours and 1, 3, 7 days) by a direct tension test on cylindrical cored specimens. The direct tensile strength was also measured as a control using the same size of specimens and testing procedures.

To prepare the cored cylinder specimens, a 100x100x500 mm beam was printed. Then, after a time gap, another 100x100x500 mm beam was printed on top. The components were then covered with damp hessian and plastic sheeting for a day before being moved to a laboratory storage area where the same curing regime was maintained up to 28 days. Six 58 mm diameter x 120 mm height cylinder specimens were cored at the middle of each bonded beam component (Figure 5).

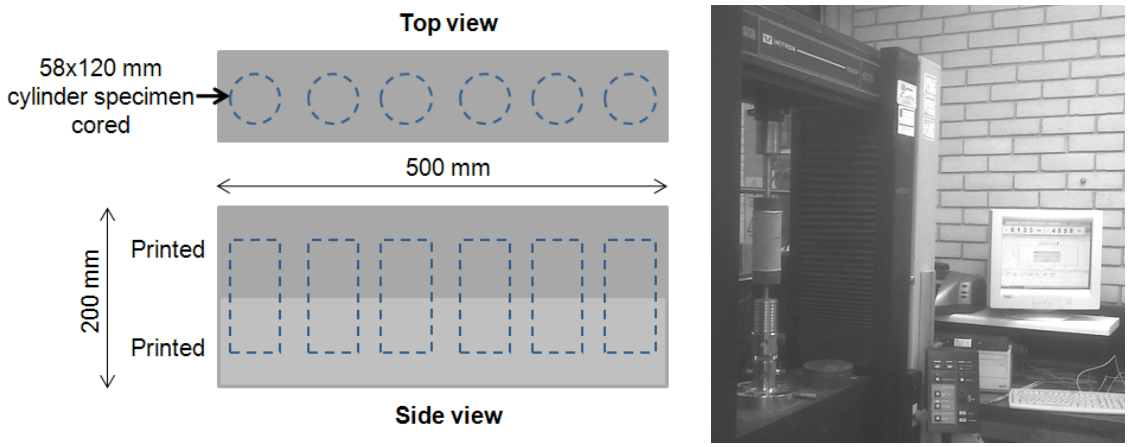

a) Coring six 58x120 mm cylinder specimens from a beam bond component

b) Testing tensile bond strength

Figure 5. Arrangement for testing tensile bond strength

The cored cylinder specimens were tested in accordance with BS EN 14488-4:2005+A1:2008 [16]. Two 58x25mm diameter x thickness steel dollies were glued to the ends of each cylinder specimen with a rapid curing, high strength adhesive.

2.3.5. Void measurement

One of the characteristics of this concrete printing process is the voids that can form between filaments (Figure 1), which might affect the hardened properties significantly. The voids in the range of 0.2 – 4.0 mm size were quantified using "Image Tool" processing and analysis software to better understand the effects on the hardened performance of the printing concrete.

Void measurement was carried out in three specimen groups of mould-cast , poor printing and good printing (Figure 6), each specimen having a 90x90 mm^2 surface.

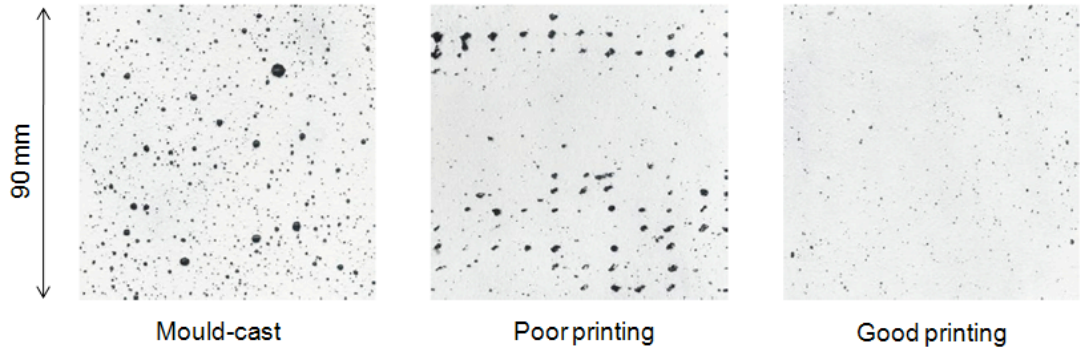

Figure 6. Three typical specimens for void measurement

Surfaces were cleaned and sprayed with a black paint. Once dry, a white paint was rolled on to reveal the voids that retained the black colour. The surface was subsequently scanned and the image transferred to a void measuring software "Image Tool" which counted the number of voids and their area.

2.3.6. Drying shrinkage

As the printing process fabricates without formwork, the surface area in contact with air is large and this could accelerate drying shrinkage due to water evaporation, and consequently increase the risk of cracking. Mould cast 75x75x229 mm beams complying with BS EN 12617-4:2002 [17] were monitored over six months in three curing conditions: water immersed, covered in damp hessian with a plastic sheet wrapped and in a climatic chamber (20^{o}C and 60% relative humidity). Each group comprised five specimens.

3. Results and Discussion

3.1. Density

The average density (mould-cast) of the optimum mix was 2,250 kg/m^3 Whilst that of well-printed specimens was a little higher at 2,350 kg/m^3 This was probably because the concrete hopper was gently vibrated before delivery of the fresh concrete, and the pipe and pump system also provided a small pressure during extrusion. A similar trend occurred in a previous study on wet-spayed mortars [23, 24]. Although this high performance printing concrete has only a sand aggregate, the density is much higher than that of ordinary mortars (1,800 kg/m^3) and sprayed mortars [23] (i.e. 1,800 – 2,000 kg/m^3 on average). The high density is also attributed to the grading and homogeneity resulting in high strengths and low shrinkage.

3.2. Compressive strength

The mould-cast cube compressive strength at 28 days was typically 107 MPa but varied with the admixtures and their dosages. The superplasticiser appeared to delay the hardening of concrete at an early age. However, as expected and also in agreement with previous work [21, 22], at 7 days and 28 days the specimens with 1-2 % superplasticiser had higher strength compared with 0.5 % superplasticiser. Without superplasticiser the fresh concrete became stiff and then could not be printed so the compressive strength was not determined. Over 1% retarder reduced

significantly the compressive strength at early ages, i.e. 1 and 7 days. Indeed 1.5-2% retarder resulted in no measurable compressive strength at 1 day. By 28 days, the retarder effect appeared to have disappeared, the compressive strengths of all mixes being approximately 100 MPa. The accelerator increased the compressive strength at one day significantly: by 70% with 3-5% and 40% with 1% accelerator. However, by 7 days, this enhancement had disappeared and by 28 days the strengths of 3-5% accelerator specimens were lower than that of 1% accelerator specimens.

Testing of printed samples in various directions relative to the layers revealed a strength from 75 to 102 MPa (see Figure 11 which includes a comparison with mould cast equivalents).

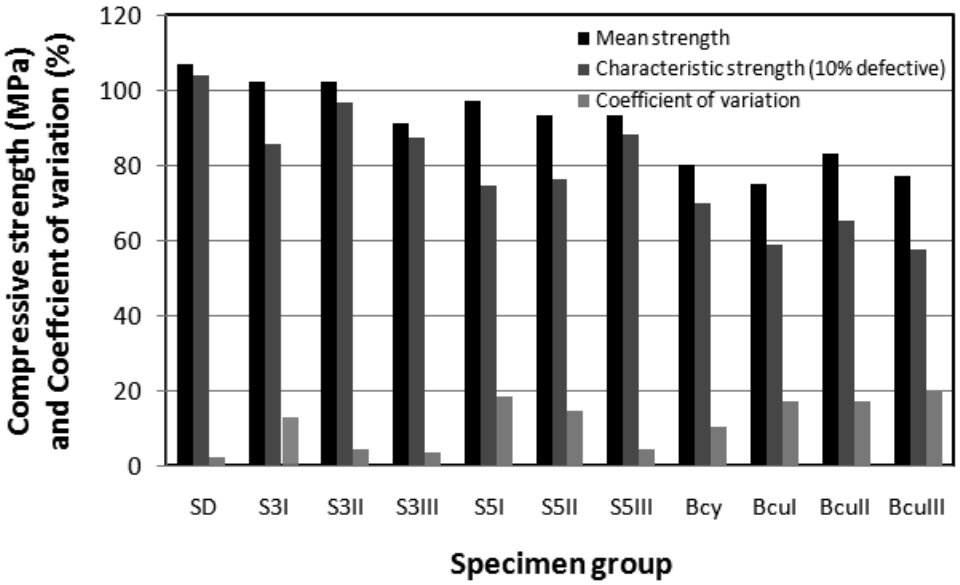

Figure 11. Equivalent 100mm cube compressive strengths of printed concretes compared with mould-cast specimens

Key:

SD – standard 100 mm mould-cast cubes

S3I, S3II, S3III – 100 mm cubes extracted from the 350x350x120 mm slab, tested in loading direction I, II and III (see Figure 2)

S5I, S5II, S5III – 100 mm cubes extracted from three 500x350x120 mm slabs, tested in loading direction I, II and III (see Figure 4)

Bcy – 58x63 mm cylinders cored from the trial curvy bench, (see Figure 3)

BcuI, BcuII, BcuIII – 63 mm cubes extracted from the trial curvy bench, tested in loading direction I, II and III (see Figure 3)

The average compressive strengths of the 100 mm cube specimens extracted from a 350x350x120 mm slab were 102 MPa in direction I (specimens 1, 2, 3) and the same in direction II (specimens 4, 5, 6). In direction III it was 91 MPa (specimens 7, 8, 9). Compared with the standard mould-cast compressive strength, the printed concrete strength was similar in directions I and II and 15% lower in direction III. The nine 100 mm cube specimens tested in the series of three 500x350x120 mm slabs, depicted in Figure 4, had an average compressive strengths of 97 MPa in direction I and 93 MPa in directions II and III. The printed strength was thus 9% lower in direction I and 13% lower in directions II and III, respectively. The results confirmed that a correctly executed extrusion process introduces relatively little anisotropy in terms of compressive strength, although it appears that loading in the plane of the layers (directions II and III) can reveal a small reduction, presumably associated with shear induced by platen friction exploiting any flaws at the bead boundaries.

However, the compressive strength reduced in the samples extracted from the print of the curvy shape (the series of fifteen 58x120 mm cylinders and fifteen 63 mm cube specimens). The equivalent cube compressive (converted using BS EN 12504:1-2009 [27] and an empirical relation [28]) varied from 75 to 83 MPa, i.e. up

30% less than the control. Additionally, the coefficients of variation of printed specimens of 17-20% were significantly higher than that of standard cubes (2%). Observation from the testing of this series revealed voids between the curved filaments that are likely to have been the cause of the lower compressive capacity.

3.3. Flexural strength

The average flexural strength of the mould-cast beams was 11 MPa (Figure 12), i.e. approximately 10%, of compressive strength, agreeing with other research on high strength concretes [29-31].

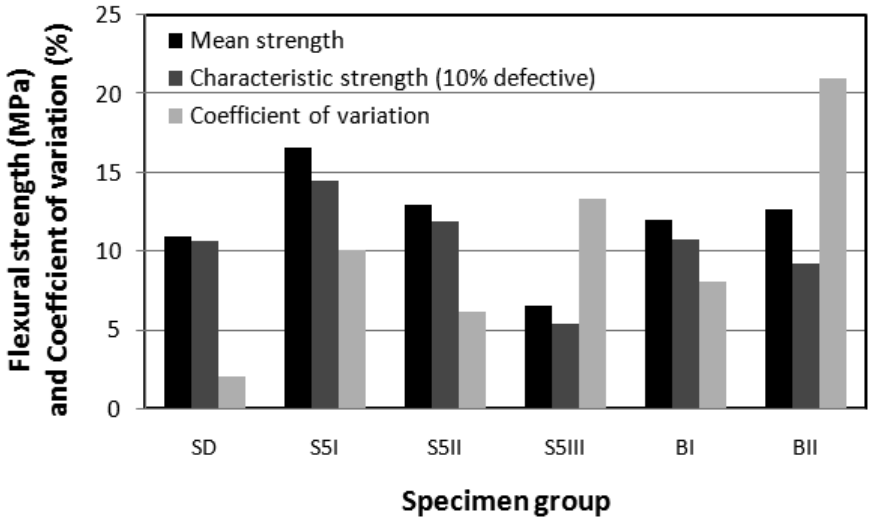

Figure 12. Flexural strengths of printed concrete compared with standard mould-cast concrete

Key:

SD – standard 500x100x100 mm mould-cast beams

S5I, S5II, S5III – 400x100x100 mm beams extracted from three 500x350x120 mm slabs, tested in loading direction I, II and III (Figure 4)

BI, BII – 220x63x50 mm beams extracted from the trial curvy bench, tested in loading direction I and II (Figure 3)

The flexural strength of printed concrete varied with testing orientation. In the series extracted from three slabs 500x350x120 mm, the strengths in loading directions I and II (16 and 13 MPa respectively), were higher than that of the standard mould cast material (11 MPa). The flexural strength is determined by the central bottom area of beam specimens where the maximum tensile stress occurs. The concrete that carried load in the testing direction I was at the bottom of the slab printed and this area was probably well-compacted. The water-binder ratio of the lower concrete layers would also have been reduced if water bled out of the base layer. The combined effect would increase the loading capacity of the lower layers resulting in a higher flexural strength. The beams tested in direction III had a much lower average strength (7 MPa). This is because of the anisotropy resulting from the printing process where, in this case, the load was applied in the plane of the boundaries between filaments and the strength is thus highly dependent on the inter-layer bond strength.

The flexural strength of smaller printed beams extracted from the curvy component (was slightly higher than the control. The mean strength of 5 beams loaded in direction I was 12 MPa and of 5 beams in direction II was 13 MPa. However these values are lower than in the same directions of the printed slabs reflecting the variation in printing quality and following the same trend as for compressive strength.

435 This is reinforced by the coefficients of variation of the printed specimens of up to
436 21% which were much larger than that of the mould-cast standard (2%).
437
438
439 ***3.4. Tensile bond strength***
440
441
442 The tensile bond strength was investigated with 11 groups of specimens with a
443 varying time gap between the older and newer part. The results are compared with
444 the direct tensile strength of similar specimens and testing procedure in Figure 13.
445
446
447 The results were quite variable, with coefficients of variation of 5 to 30%. This was
448 expected given the nature of the layered extrusion process and the well established
449 more general discussions concerning measurement of direct tensile strength [29] and
450 tensile bond testing of concrete repairs [32]. It is thought that such specimens are
451 more seriously affected by non-uniform shrinkage in comparison with other types of
452 test specimens.
453
454

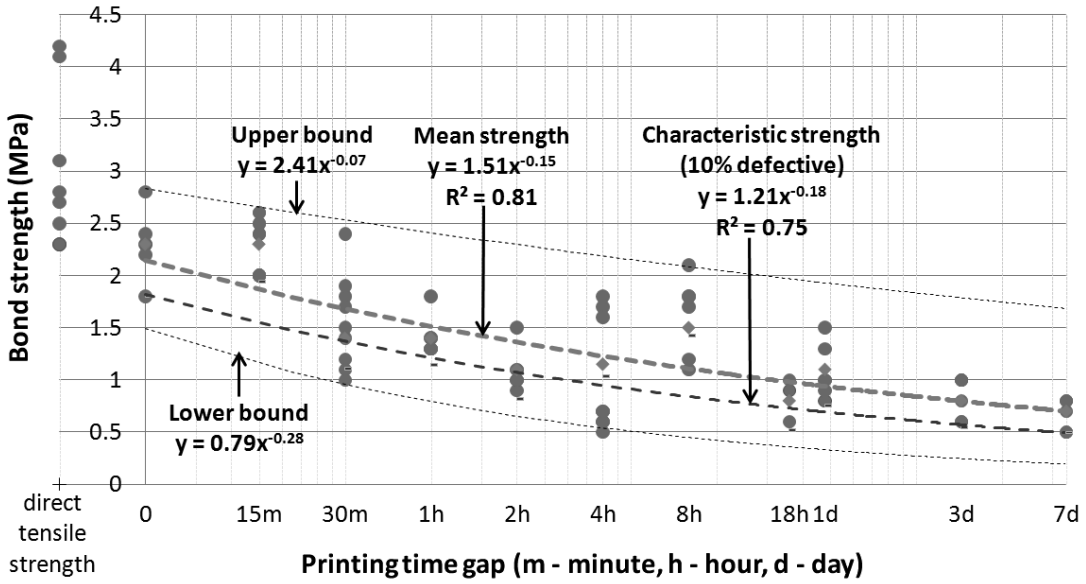

455

456 Figure 13. Variation of tensile bond strength with printing gap and comparison with

457 direct tensile strength

458

459

460 The failure stress was lower than the average tensile strength of 3.0 MPa, reducing

461 on average from 2.3 MPa with printing time gaps of 0 and 15 minutes to 0.7 MPa for

462 the 7 day gap. The specimens with a 0 and 15 minute time gap failed in the material

463 (Figure 14a) and thus the bond strength could not be determined but is higher than

464 the measured values.

465

466

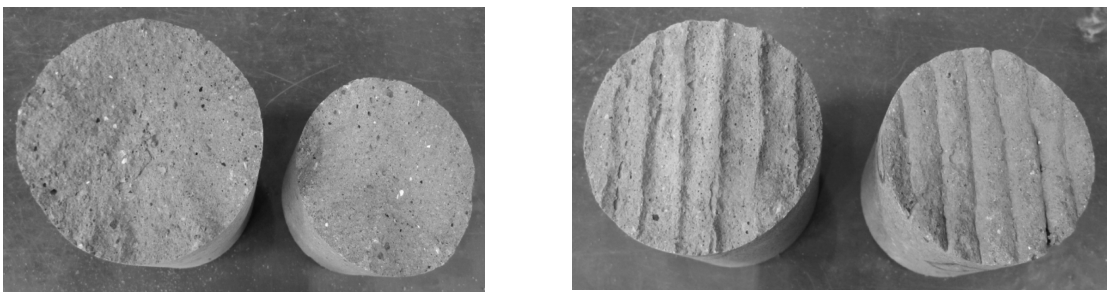

a) 15 minute gap specimen b) 4 hour gap specimen

467 Figure 14. Failure mode (broken surfaces) of tensile bond specimens

468

All specimens with a gap over 15 minutes failed at the interface between older and newer parts (Figure 14b). Between a 30 minute and 7 day time gap the average bond strength was 53% and 77% lower than the control. This reduction with increasing gap in printing time was expected as the adhesion reduced. However, most of the results comfortably exceeded the Concrete Society recommended minimum bond strength of 0.8 MPa [23], and are well above the 0.4 to 0.9 MPa in a case study of a high performance concrete bridge deck overlay [33]. They are similar to published bond strengths of repair mortars and concretes of 0.8 to 2.3 MPa [23, 32, 34]. The trend lines suggest that characteristic bond strengths of 0.8, 1.0 and 1.2 MPa will be achieved with time gaps of 8, 3 and 1 hours respectively. A more demanding 1.5 MPa would restrict the printing time per layer to around 15 minutes.

3.5. Void structure

The anisotropy affecting the hardened properties including the compressive, flexural and tensile bond behaviour was supported by the results of the void measurement. These revealed 3.8% voids (0.2 – 4.0 mm size) in mould-cast specimens whilst 4.8% formed in the poorly printed concrete and only 1.0% voids in the well printed concrete. Respectively, the density results were 2,250, 2,260 and 2,350 kg/m^3 for mould-cast, poor printing and good printing. Although the void content of the poorly printed concrete (4.8%) was greater than that of the mould-cast (3.8%) the density was higher, implying a higher density. The content of voids less than 0.2 mm diameter in the printed concrete is likely to be smaller than that of mould-cast concrete.

The distribution of voids in the three concrete groups, Figure 15, clearly shows that the area of small voids (0.2 – 1.6 mm) in mould-cast concrete was very much greater than that of both poor and good printing concrete. The poorly printed had more large voids (1.6 - 4.0 mm) compared with mould-cast concrete and are mostly located between printed filaments (Figure 6). Once these were eliminated by correctly controlling the printing path and concrete rheology, the density increased as seen in the well printed concrete (2,350 kg/m^3) that is representative of the specimens prepared for the other hardened property tests. The distribution of voids in good printing concrete agreed well with this as the area of 0.2 – 4.0 mm voids was significantly lower than both mould-cast and poor printing concrete.

Whilst the tests reported here are not extensive they provide important insights into the nature of this extrusion process and the influence on the structure of the resulting matrix and hence mechanical performance.

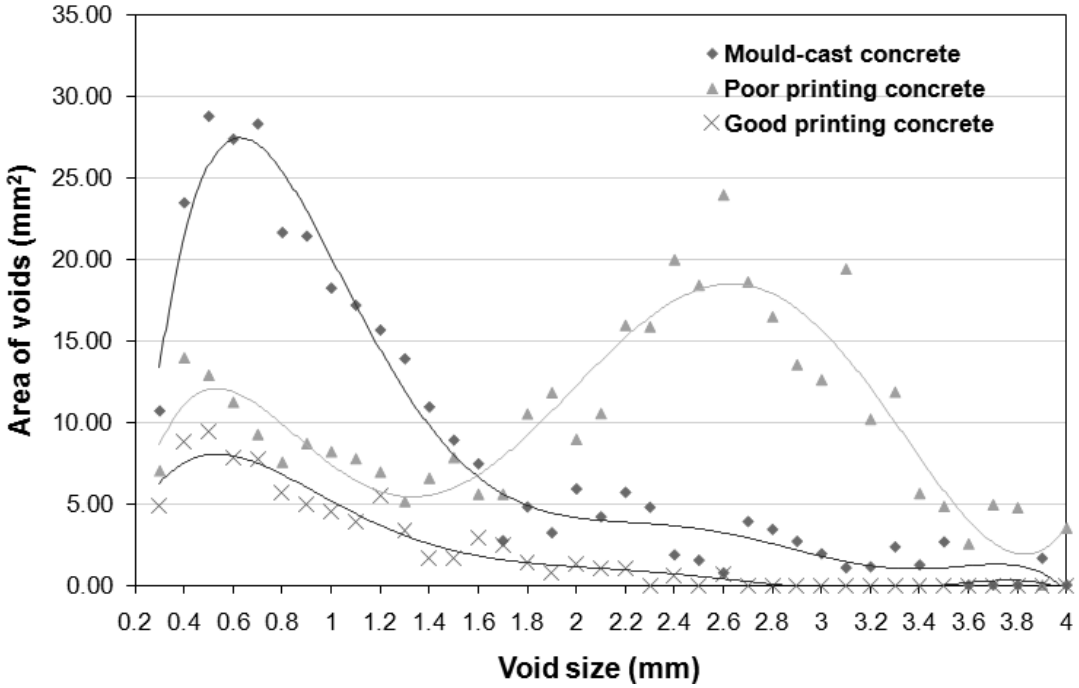

515

516 Figure 15. Distribution of voids in three concrete groups

517

518

519 ***3.6. Drying shrinkage***

520

521

522 As expected, the concrete cured in water shrank the least. It expanded up to 67
523 microstrain in first two days and then shrank to 177 microstrain by 28 days.
524 Thereafter the shrinkage rate noticeably reduced with only 62 microstrain between 30
525 and 180 days. (Figure 16. The influence of damp hessian was monitored in two
526 phases. During the first 60 days it was watered and wrapped in plastic sheeting so
527 the relative humidity was around 100% but the temperature varied in a range of 15 to
528 25^{o}C depended on the ambient conditions. The shrinkage of 252 microstrain by 70
529 days was relatively low. In the second phase when the hessian was not watered and
530 the plastic sheeting removed, the shrinkage rate increased from 70 to 90 days (408
531 microstrain), then gradually slowed to 570 microstrain at 184 days. The concrete in

the climatic chamber at a consistent 20°C and 60% relative humidity shrank quickly in first 30 days by 597 microstrain then gradually slowed to 855 microstrain at 189 days.

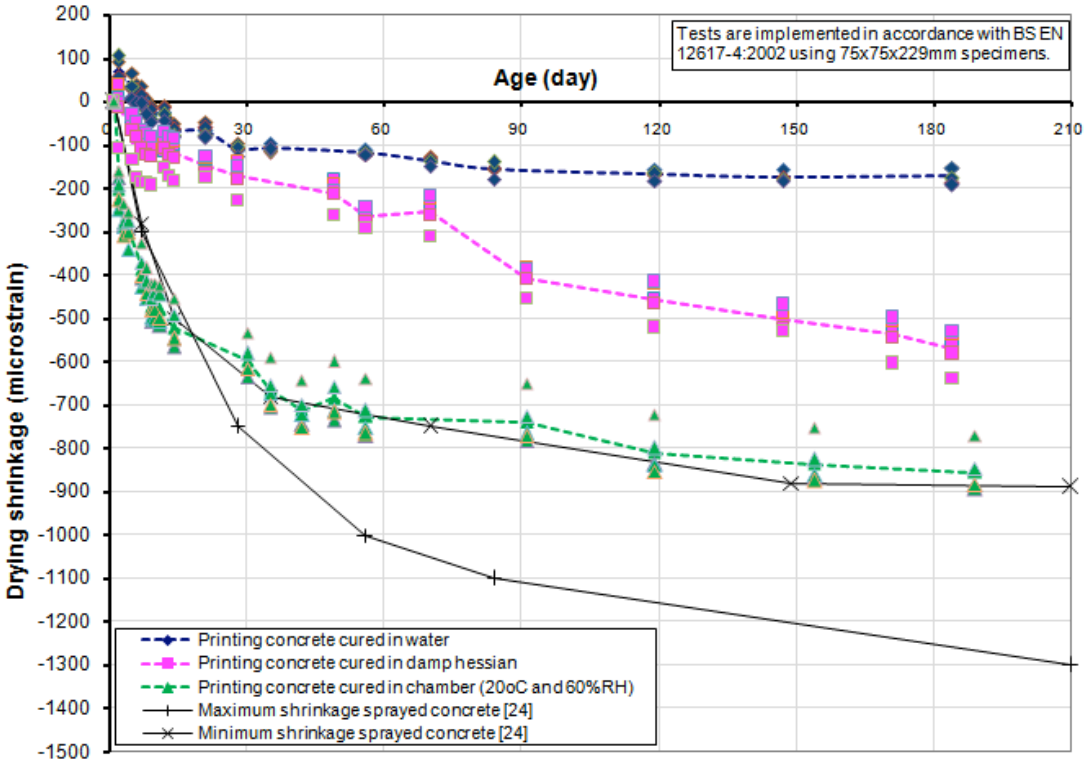

Figure 16. Drying shrinkage in three curing conditions with comparison to sprayed concretes

The higher shrinkage, by a factor of 3-4 times larger than that cured at 100% relative humidity, agrees reasonably well with the research by Bissonnette et al. [35] who observed the influence of relative humidity on the drying shrinkage of a mortar and obtained the results of approximately 300, 800 and 1400 microns for the specimens cured in 92, 75 and 48% relative humidity, respectively. Brooks et al. [36] also found greater shrinkage in 30 MPa compressive strength mortar specimens cured under plastic sheeting (approximately 2,200 microns) compared with water (approximately

548 1,000 microns). The results are thus as would be expected of cementitious system
549 sensitive to changes in relative humidity, which disturb the equilibrium between
550 adsorbed water and vapour pressure [37].
551
552
553 The shrinkage in all three conditions was notably lower than that of sprayed mortars
554 [23, 24] considered to be low shrinkage materials, when cured at 20^{o}C and 50%
555 relative humidity. The optimum particle grading, low water/binder ratio and fly ash
556 addition thus appeared to be helpful in lowering the shrinkage of the high
557 performance printing concrete. This is a notable advantage for a manufacturing
558 process without formwork where the complete surface of components is exposed.
559
560
561 **4. Conclusions**
562
563
564 A high-performance concrete has been successfully developed for a digitally-
565 controlled printing process which can build architectural and structural components
566 without formwork. The concrete in the mould-cast state had high strengths (107 and
567 11 MPa compressive and flexural strength respectively), low drying shrinkage and a
568 density of 2,250 kg/m^3. The printing process increased the density up to 2,350 kg/m^3,
569 although, as anticipated, the layering process can introduce small linear voids in the
570 interstices between the extruded filaments. The gentle vibration of concrete container
571 and the small pump pressure in the extrusion process probably reduced the volume
572 of voids, resulting in the increase in density. Furthermore, poor printing could result in
573 a lower density (2,260 kg/m^3) with 1.6 – 4.0 mm voids. located principally at the
574 intersection of filaments
575

The hardened properties were inevitably affected by any anisotropy in the layered structure of freeform components. Up to 30% reduction in compressive strength was observed in a curvy-shape full-scale bench structure. The potential improvement is implied by the higher strengths of around 91-102 MPa found in the specimens extracted from straight-line printed slabs. Here the reduction was only 5-15%, depending on the orientation of the loading relative to the layers, the lowest strengths occurring as would be expected when loading in planes parallel to the layers.

In terms of tensile properties, the flexural strength was significantly higher (13-16 MPa) than the mould-cast control (11 MPa) when tension was aligned with the extruded filaments. However, as expected, the flexural strength was significantly reduced when loaded to cause tension between (perpendicular) the layers (by up to 36%) but still high relative to conventional precast concretes at 7 MPa. A similar trend was observed in the measurement of direct tensile strength, reducing from 3.0 MPa in the mould-cast control to 2.3 MPa, the difference between the indirect and direct values following well-established behaviour.

The bond strength between the layers of printed concrete is perhaps the critical mechanical property of material produced by an AM process, creating potential flaws between extrusions that induce stress concentrations. This is highly dependent on the adhesion which is a function of the time between extrusions. There is a careful balance required, as with sprayed concretes, keeping the materials sufficiently open for adhesion, but developing sufficient rigidity to support its self-weight. The optimised mix contained appropriate proportions of superplasticizer and retarder.

The tensile bond strength inevitably reduced as the printing gap between ayers increased. Where this was kept to 15 minutes the bond was greater than the tensile capacity of the material. A gap of 30 minutes or more resulted in bond failure at the interface and a relationship between characteristic bond strength and time has been established.

In macro terms, a variety of freeform building components were printed, including a large-scale curvy bench with weight of approximately 1 tonne [7, 8]. Whilst drying shrinkage of such parts is inevitably a concern, the data indicates acceptable levels when good curing is provided. The research has thus demonstrated the potential of concrete printing as a viable new production process that can introduce greater geometric freedom into the design process as well as offering a novel means of manufacture that could avoid the need to mass produce identical concrete parts with limited numbers of variants. Further research is required to assess the structural behaviour of such components under simulated service conditions as well as to establish their durability, particularly in relation to any adverse effects of the layering process.

Acknowledgements

This project was funded by the Engineering and Physical Sciences Research Council under grant EP/E002323/1 through the IMCRC at Loughborough University. The authors acknowledge the supply of materials from Hanson Cement, Weber (St Gobain) and BASF and the assistance in designing the freeform components from

632 Foster & Partners and Buro Happold. We are also grateful for the laboratory
633 assistance of John Webster, Gregory Courtney, Harriet Mather, Jonathan Hales and
634 David Spendlove.
635
636
637 **References**
638
639
640 [1] R. A. Buswell, R. C. Soar, A. G. F. Gibb, T. Thorpe, Freeform construction: Mega-
641 scale rapid manufacturing for construction, Automation in Construction, 16 (2007)
642 224-231.
643 [2] S. Lim, T. Le, J. Webster, R. Buswell, S. Austin, A. G. F. Gibb, T. Thorpe,
644 Fabricating construction components using layer manufacturing technology,
645 Proceedings of International Conference on Global Innovation in Construction,
646 Loughborough, UK, 2009, pp. 512-520.
647 [3] H. Okamura, M. Ouchi, Self-compacting concrete, Journal of Advanced Concrete
648 Technology. 1 (2003) 5-15.
649 [4] RILEM Technical Committee, Final report of RILEM TC 188-CSC “Casting of self
650 compacting concrete“, Materials and Structures, 39 (2006) 937-954
651 [5] S. A. Austin, P. Robins, C. I. Goodier, The rheological performance of wet-
652 process sprayed mortars, Magazine of Concrete Research, 51 (1999) 341-352.
653 [6] S. A. Austin, P. Robins, C. I. Goodier, Construction and Repair with Wet-Process
654 Sprayed Concrete and Mortar, Technical Report 56, The Concrete Society, UK,
655 2002, p. 44.
656 [7] T. T. Le T, S. A. Austin, S. Lim, R. Buswell, A. G. F. Gibb, T. Thorpe, Mix design
657 and fresh properties for high-performance printing concrete, Materials and Structures
658 (accepted in June 2011).

659 [8] T. T. Le T, S. A. Austin, S. Lim, R. Buswell, A. G. F. Gibb, T. Thorpe, High-
660 performance printing concrete for freeform building components, Proceedings of
661 International Fib Symposium on Concrete Engineering for Excellence and Efficiency,
662 Prague, Czech Republic, 2011, pp. 499-502.
663 [9] B. Khoshnevis, D. Hwang, K. Yao, Z. Yeh, Mega-scale fabrication by contour
664 crafting, International journal of Industrial and System Engineering 1 (2006) 301–320.
665 [10] Enrico Dini. *"D_Shape."*, http://www.d-shape.com, accessed on 05th October
666 2011.
667 [11] A. M. Evans, R. I. Campbell, A comparative evaluation of industrial design
668 models produced using rapid prototyping and workshop-based fabrication
669 techniques, Rapid Prototyping Journal, 9 (2003) 344–351.
670 [12] J. Pegna, Exploratory investigation of solid freeform construction, Automation in
671 Construction, 5 (1997) 427–437.
672 [13] World Technology Evaluation Center, Inc., Additive / Subtractive manufacturing
673 research and development in Europe, WTEC Panel report, 2004, p. 154. [14] British
674 Standards Institution, BS EN 12390-3:2009 Testing hardened concrete -
675 Compressive strength of test specimens, Milton Keynes, UK, 2009, p. 15.
676 [15] British Standards Institution, BS EN 12390-5:2009 Testing hardened concrete -
677 Flexural strength of test specimens, Milton Keynes, UK, 2009, p. 11.
678 [16] British Standards Institution, BS EN 14488-4:2005+A1:2008 Testing sprayed
679 concrete - Bond strength of cores by direct tension, Milton Keynes, UK, 2008, p. 7.
680 [17] British Standards Institution, BS EN 12617-4:2002 Products and systems for the
681 protection and repair of concrete structures. Test methods. Determination of
682 shrinkage and expansion, Milton Keynes, UK, 2002, p. 14.
683 [18] British Standards Institution, BS EN 12390-7:2009 Testing hardened concrete -
684 Density of hardened concrete, Milton Keynes, UK, 2009, p. 10.

685 [19] S. Erdogdu, Effect of retempering with superplasticizer admixtures on slump loss
686 and compressive strength of concrete subjected to prolonged mixing, Cement and
687 Concrete Research, 35 (2005) 907-912.
688 [20] V. Morin, F. C. Tenoudjia, A. Feylessoufib, P. Richard, Superplasticizer effects
689 on setting and structuration mechanisms of ultrahigh-performance concrete, Cement
690 and Concrete Research, 31 (2001) 63-71.
691 [21] American Concrete Institute, ACI 212.4R-93 (Reapproved 1998) Guide for the
692 Use of High-Range Water-Reducing Admixtures (Superplasticizers) in Concrete,
693 1998, p. 10.
694 [22] UK Cement Admixtures Association, Admixture Technical Sheet – ATS 2
695 Superplasticising / High range water reducing, 2006, p. 5..
696 [23] S. A. Austin, P. Robins, C. I. Goodier, The performance of hardened wet-process
697 sprayed mortars, Magazine of Concrete Research, 52 (2000) 195-208.
698 [24] C. I. Goodier, S. A. Austin, P. Robins, Low-volume wet-process sprayed
699 concrete: hardened properties, Materials and Structures, 41 (2008) 99-111.
700 [25] UK Cement Admixtures Association, Admixture Sheet – AS 3 Set Retarding. Set
701 Retarding / Water Reducing / Plasticising. Set Retarding / High Range Water
702 Reducing / Superplasticising, 2006, p. 4.
703 [26] UK Cement Admixtures Association, Admixture Sheet – ATS 4 Accelerating
704 admixtures, 2006, p. 4..
705 [27] British Standards Institution, BS EN 12504-1:2009 Testing concrete in structures
706 Part 1: Cored specimens — Taking, examining and testing in compression, 2009, p.
707 8.
708 [28] J. R. Del Viso, J. R.Carmona J R, G. Ruiz, Shape and size effects on the
709 compressive strength of high-strength concrete, Cement and Concrete Research, 38
710 (2008) 386–395.
711 [29] A. M. Neville, Properties of concrete, Longman group limited, England, UK,
712 1995.

713 [30] T. T. Le, Ultra high performance fibre reinforced concrete paving flags, PhD
714 thesis, University of Liverpool, UK, 2008, p. 405.
715 [31] S. Bhanjaa, B. Sengupta, Influence of silica fume on the tensile strength of
716 concrete, Cement and Concrete Research, 35 (2005) 743-747.
717 [32] S. A. Austin, P. Robins, Y. Pan, Tensile bond testing of concrete repairs,
718 Materials and Structures, 28 (1995) 249-259.
719 [33] Department of Transportation, United States, Tensile bond strength of a high
720 performance concrete bridge deck overlay - Field test report, Federal Highway
721 Administration, Office of Pavement Technology, Washington, USA, 2000, p. 10.
722 [34] K. H. Hindo, In-plane bond testing and surface preparation of concrete, Concrete
723 International, 12 (4) (1990) 46-48.
724 [35] B. Bissonnette, P. Pierre, M. Pigeon, Influence of key parameters on drying
725 shrinkage of cementitious materials, Cement and Concrete Research, 29 (1999)
726 1655–1662.
727 [36] J. J. Brooks, B. H. Abu Bakar B H, Shrinkage and creep of masonry mortar,
728 Materials and Structures, 37 (2004) 177-183
729 [37] K. Kovler, S. Zhutovsky, Overview and future trends of shrinkage research,
730 Materials and Structures, 39 (2006) 827–847.